International Symposium
On Turbulence and Shear Flow
Phenomena (TSFP-9)
June 30 - July 3, 2015 *Melbourne, Australia*

CONTROL OF BACKWARD FACING STEP FLOW USING NS-DBD PLASMA ACTUATORS

Giuseppe Correale
Department of Aerospace Engineering
Delft University of Technology
Kluyverweg 1, 2629 HS, Delft, The Netherlands
g.correale@tudelft.nl

Marios Kotsonis
Department of Aerospace Engineering
Delft University of Technology
Kluyverweg 1, 2629 HS, Delft, The Netherlands
m.kotsonis@tudelft.nl

ABSTRACT

An experimental investigation was carried out on the effect of unsteady periodic pulsed perturbation on a separated laminar shear layer. Time resolved PIV was used to characterize a backward-facing step flow ($Re_h = 3600$), periodically actuated by a nanosecond DBD plasma actuator. The forcing frequency ranges between 20 and $200Hz$, and it is the only parameter investigated.

Results indicate a decrease of reattachment length with increasing frequency, reaching a minimum at $160Hz$. Frequency analysis and linear stability theory have shown that a perturbed flow adjusts itself to a new stable state. Proper orthogonal decomposition (POD) has revealed that the effect of a pulsed perturbation is to redistribute energy among modes. Therefore, a pulsed periodic actuation of a laminar shear layer promotes the development of large structures due to inviscid-viscous interaction. These convect downstream resulting in a mean flow deformation which causes a change of stability. New unstable frequencies are excited and promote the redistribution of energy among modes. This ultimately affects the efficiency of actuation in promoting transition from laminar to turbulent flow.

INTRODUCTION

Controlling a fixed-point separated flow cause by surface aberrations or adverse pressure gradients is very important topic for many engineering applications. This generated a great number of studies numerical, theoretical and experimental (Michalke, 1965; Armaly *et al.*, 1983; Huerre & Monkewitz, 1985; Blackburn *et al.*, 2008) and many different flow control techniques for fixed-point separation were developed (Bhattacharjee *et al.*, 1986; Hasan, 1992; Roos *et al.*, 1986; Kim *et al.*, 1980). To some extend, backward-facing step flow mimics such scenario.

Armaly *et al.* (1983) observed a reattachment length after the step being dependent on the Re number. More specifically, a turbulent separated flow experiences a shorter separation length, being more energetic so capable of afford a more efficient expansion after the step.

From a numerical point of view, it is found in literature (Huerre & Monkewitz, 1985; Balsa, 1988; Lie & Riahi, 1988) that BFS flows are unstable at very low Renumber, i.e. few millimetre after the step, even at very low free stream velocities. Kaiktsis *et al.* (1991) comparing numerical prediction and experimental data found a discrepancy attributed to the distortion of flow. This phenomenon delivers a change of the stability of the flow itself. It seems that a shear layer transitioning from laminar to turbulent would adapt itself to new state, so changing its own stability. Balsa (1988) have studied the receptivity of free shear layer subject to pulsed periodic excitations. They postulated that co-flowing shear layers are convectively unstable and spatial instability modes always arise in them because of periodic excitation. Such flow scenario is identical to the one investigated in this work. Therefore, results from Balsa (1988) have been used in order to validate the in-house LST solver used in this work. Kaiktsis *et al.* (1996) have investigated the stability of a backward facing step using a bi-dimensional Direct Numerical Simulation together with local and global stability analysis under impulsive forcing. They found that sustained external perturbation can make the stability of a shear layer time-dependent, i.e. make the flow globally unstable.

Several attempt of flow control over a backward facing step are present in literature, mainly for turbulent inflow conditions (Bradshaw & Wong, 1972; Kim *et al.*, 1980; Bhattacharjee *et al.*, 1986; Roos *et al.*, 1986; Chun & Sung, 1996). Few example of laminar separated flow control are present (Roos *et al.*, 1986; Bechert & Stahl, 1988; Hasan, 1992; Wengle *et al.*, 2001). It seems important to make distinction between the kind of inflow boundary layer since there are evidences of an effective flow control when turbulent inflow boundary layer is excited with a frequency equal to the naturally most unstable frequency present into the shear layer (Chun & Sung, 1996). Such result looks not to be consistent when the inflow condition is laminar. The nature of the stability of a free laminar shear layer under the effect of controlled periodic perturbations seems to be strongly coupled with the frequency of actuation itself

(Hasan, 1992), changing the stability of the base flow (Kaiktsis *et al.*, 1996).

As already stated at the beginning of this introduction, the importance of designing flow control strategies and techniques capable of controlling separated shear layers is of primary importance in many engineering applications. Although a vast selection of previous work has been directed towards this goal, several aspects remain unclear. More specifically, the effect of actuation is producing in many cases a mean flow deformation effect which has significant influence on the development of new stability characteristics of the flow. A simple question one might pose is: "Should the optimal actuation frequency be based on the stability characteristics of the forced or non-forced flow?". Similar considerations involve the actual spatial location of the forcing. In most engineering applications the actuator is envisaged upstream of the breakdown region. Yet the forced instability modes will result in breakdown further downstream where different stability characteristics might apply. A second question would be: "Should the optimal control frequency be based on the stability of the flow at the actuator position, or further downstream?".

In order to answer these questions flow over a BFS is experimentally investigated. Such geometry is selected due to its capability of mimicking the topology of massively separated flows such as the ones typically encountered on airfoils at large angles of attack. The stability of a laminar flow past a BFS under the effect of periodic pulsed perturbations is characterised with the use of time resolved PIV. A super-elliptical leading edge assures the development of a stable laminar boundary layer upon the surface of the at plate (Lin *et al.*, 1992), with the subsequent downstream formation of a free shear layer. A flush mounted ns-DBD plasma actuator is selected in order to introduce into the flow a controlled pulsed and periodic thermal disturbance (Correale *et al.*, 2014). Time resolved velocity measurements allow frequency as well as POD analysis. Thus, investigation on the dependency of the actuation frequency coupled with the energy redistribution between the unstable modes for each actuated as well as non-actuated case is performed. LST is applied by solving the Orr-Sommerfeld equation with an in-house developed solver (Van Ingen & Kotsonis, 2011).

EXPERIMENTAL SET-UP

Experiments were carried out in a low speed open loop facility with a maximum free stream velocity of $40m/s$ with a free stream turbulence intensity of about 0.1% at maximum speed. The model used for the experiments was a flat plate with a super-elliptical leading edge and a backward facing step 150 mm downstream from the leading edge. A groove allows flush mounting a nanosecond DBD plasma actuator, as shown in figure 1.

Two components planar Time Resolved Particle Image Velocimetry (2C-TR-PIV) measurement technique is employed. The used camera (LaVision Imager pro HS 4M) has a $4megapixel$ ($2016\times2016pixels$), $12bit$ CCD sensor. A Nikon $105mm$ macro objective was used, set at $f^{\#}=5.6$. The light source was a Darwin-Duo laser by Quantronix, with an average output of $80W$ at $2kHz$. A combination of cylindrical and spherical lenses were used in order to form a light sheet approximately $0.8mm$ thick, located at the midspan of the model. Seeding was provided by a SAFEX Twin-Fog smoke generator device yielding particles of about $1m$ diameter. The field of view lies in the x-y plane (figure 1), covering about $12mm$ upstream the BFS and $100mm$ downstream the step resulting in a window of $112\times32mm^2$. Double frame images were acquired at a frequency of $2kHz$ for $2.5s$. The flow velocity was kept at about $5m/s$ resulting in $Re_h=3600$. The final interrogation window $16pixel^2$ with 75% overlap. Final vector density was $3.375vector/mm$.

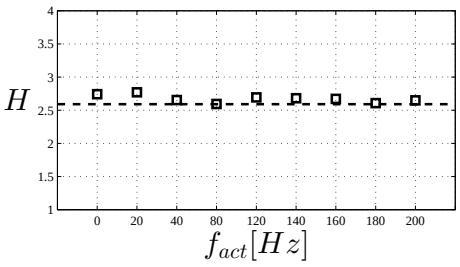

Figure 2. Shape factor H (□ symbols) for all the investigated cases. A dashed horizontal line represents the theoretical value of H for the Blasius solution. f_{act} indicates the frequency of flow actuation.

RESULTS

Frequency of flow actuation is the only parameter investigated. Pulse voltage is kept constant at $10kV$. Frequencies investigated are $20,40,80,120,140,160,180$ and $200Hz$. Acquisitions are carried out at $2kHz$ for $2.5s$. With such acquisition configuration a set of 5000 double frames are acquired for each case under study. In order to avoid low-frequency oscillation of the mean flow typically associated with the seize of actuation (Rist *et al.*, 1996; Marxen, 2005) the flow was kept actuated for the whole duration of the PIV acquisition. Free stream velocity was kept constant at about $5m/s$ resulting in a Reynolds number based on the step height of $Re_h=3600$.

Base Flow In figure 2 the shape factor H is calculated at $x/h=0$ for all the investigated cases. A black horizontal dashed line represents the value for laminar flow (Blasius). For all the investigated cases H is always above the value typical for laminar flows, thus condition of laminar separation is kept.

In figure3 the Power Density Spectrum (PSD) is reported measured at $y/h=0$ at three downstream locations, $x/h=3,4$ and 5 as function of Strouhal number based on momentum thickness (calculated at $x/h=0$).

The most amplified non-dimensional frequency corresponds to $St_\theta=0.012$, as reported in literature (Eaton & Johnston, 1981; Hasan, 1992). Such value corresponds in physical space to a frequency of about $120Hz$.

In figure 4a the stability diagram calculated for the base flow is presented. The Orr-Sommerfeld equation is solved by means of Chebyshev polynomials (Orszag, 1971) via a Matlab code developed in-house(Van Ingen & Kotsonis, 2011). The code had been validated inputting a well-known hyperbolic tangent velocity profile and results have been compared to literature (Monkewitz & Huerre, 1982; Huerre & Monkewitz, 1985; Balsa, 1988; Lie & Riahi, 1988). For

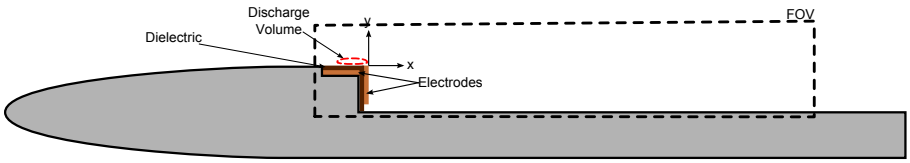

Figure 1. Model used for experiment and field of view to scale. Discharge volume not in scale.

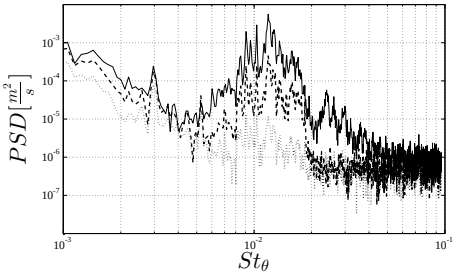

Figure 3. Distribution of PSD of the base ow as function of non-dimensional frequency. Probes located at $y/h = 0$ and $x/h = 3$ (dotted line), $x/h = 4$ (dashed line) and $x/h = 5$ (solid line).

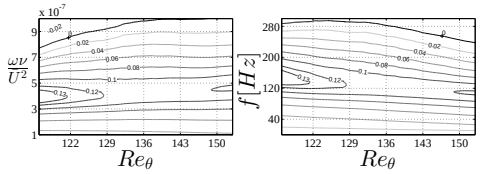

Figure 4. Left. Calculated stability diagram for base flow in non-dimensional scales. Right. Calculated stability diagram for base flow as function of physical frequency (f).

calculation, local velocity profile, Reynolds number and the non-dimensional frequency ω were scaled on the momentum thickness (as defined in Lie & Riahi (1988) and the edge velocity at each x location.

A thicker black line indicates the curve of neutral stability. It is apparent that theoretically this base flow is unstable already at very low Reynolds number (Michalke, 1965; Balsa, 1988; Lie & Riahi, 1988). In figure 4b it is possible to appreciate that the most naturally unstable frequency is in the order of $120Hz$, value close to the one experimentally observed via FFT analysis.

Reattachment length Reattachment point is defined as in literature (Hasan, 1992), i.e. the location were the mean flow velocity closer to the bottom wall approaches to zero. Given the finite spatial resolution of the PIV measurements, the exact reattachment point was extrapolated by linear data interpolation. In figure 5 the trend of reattachment length in function of frequency of actuation is shown. As already observed in figure 4, the reattachment length of the non-actuated case is about 8 times the step height (h), as found in literature for this Re_θ (Armaly *et al.*, 1983; Hasan, 1992). Interestingly enough, it is possible to see that the trend of flow reattachment reaches a minimum around a frequency of actuation of $160Hz$, frequency far from the most

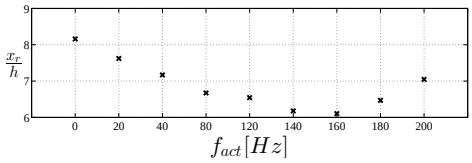

Figure 5. Reattachment length as function of forcing frequency (f_{act}).

unstable frequency measured within the base flow.

Frequency analysis A frequency analysis performed on the actuated cases by means of FFT reveals a functional relationship between forcing frequency and spectral content of the developed flow. In figure 6 PSD of horizontal velocity fluctuations is shown for all forcing cases. For each case signals in two probe position downstream the step were considered, at $x/h = 1$ (dotted line) and $x/h = 3$(solid line) respectively in the streamwise direction, at $y/h = 0$.

It is noted that, for all the cases, peaks corresponding to the actuation frequencies and their sub or super harmonics are distinguishable. For the case of $80Hz$, two main peaks appear: at $80Hz$ and at $160Hz$. Both peaks are about $40Hz$ apart from the most unstable frequency of the base flow, i.e. $120Hz$. Even if the forcing is actually $80Hz$, the most energetic peak appears to be at $160Hz$, i.e. a super-harmonic of the forcing frequency. This behaviour indicated that the natural stability of the actuated flow is changed, shifted forward higher frequencies.

The case of actuation frequency of $120Hz$, in figure 6, reveals only two peaks clearly distinguishable while most amplified frequency is close to the one found in the base flow, i.e. $120Hz$. Same dominant peak is found for actuation frequency of $20Hz$ and $40Hz$ (both sub-harmonics of $120Hz$), as result of a resonance effect between flow structures naturally developed into the flow and actuation forcing (Hasan, 1992; Chun & Sung, 1996).

The cases of actuation frequency of 140 and $180Hz$ show only one peak corresponding to the actuation frequency. Special attention is required to analyse the case of $160Hz$. For this case, super harmonics of the forcing frequency are excited indicating an enlargement of the unstable frequency range of the flow under control up to $480Hz$. It is interesting to note that the most energetic peak for this case corresponds to the most energetic mode among all actuated cases under investigation, even if the actuator energy input is always the same. This indicates that the forcing frequency of 160 Hz is very close to the most amplified frequency of the actuated flow, which is considerably different than the one of the base flow. This is confirmed by the most successful reduction of the reattachment length induced by this actuation frequency, as figure 5 shows.

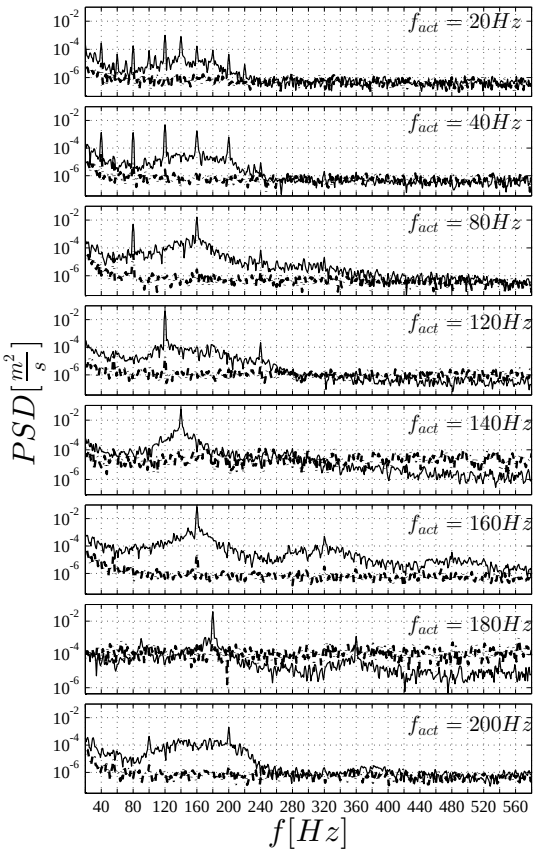

Figure 6. PSD of the horizontal velocity fluctuations versus physical frequency (f). Probe locations at $x/h = 1$ (dotted line) and $x/h = 3$ (solid line) at $y/h = 0$. f_{act} denotes frequency of actuation.

Overall, it is apparent that the stability of the actuated flow is changed compared to the base flow. For the majority of actuation frequencies an increase of the unstable region within the frequency domain is observed, until the case of $160Hz$ forcing frequency.

This indicates that the "stability" of a periodically pulsed actuated flow is a strong function of the forcing frequency itself. The periodic pulsed perturbations which are convectively amplified downstream develop in large scale structures and promote transition form laminar to turbulent flow, in turn modifying the separated region (see figure 5). Due to the inviscid-viscous interaction (Smith, 1986; Sychev, 1998) the mean flow downstream of the transition location changes the overall pressure distribution across the field of motion affecting the flow also upstream. Therefore, a mean flow deformation is caused, which consequently changes the stability of the flow under control (Marxen & Rist, 2010).

Proper Orthogonal Decomposition The stability of a flow is a function of the energy distribution among its infinite modes (Couplet *et al.*, 2003; Gudmundsson & Colonius, 2011). Thus, modal energy is investigated via POD analysis of the time resolved PIV data, using the snapshot method (Sirovich, 1987*a*,*b*,*c*) over the whole set of data, i.e. 5000 realisations. Each mode is characterised by its own energy content, and can be described as a linear combination of snapshots. Thus, snapshots of velocity fluctuations can be used to solve an eigenvalue problem and determine spatial modes of energy distribution. The calculated eigenvalues associated to each mode represent the kinetic energy of the mode itself relatively to the total kinetic energy of all calculated modes. Moreover, the modes are ordered in function of their energy content.

Figure 7 shows the normalised energy content of the first ten POD modes (E_m) relative to the total fluctuation energy (E_{tot}) for all tested cases. It is possible to note in all the cases that groups of two or three eigenvalues have similar energy content. These modes are coupled, i.e. their correspondent eigenvector interact with each other (Farrell, 1988; Couplet *et al.*, 2003). In general, coupled modes are characteristics of periodic flow phenomena as for the case of Karman shedding (Deane *et al.*, 1991; Van Oudheusden *et al.*, 2005). In the same manner, when an eigenvalue is uncoupled it represents non-periodic flow structures like the one produced by a flapping laminar separation bubble (Price *et al.*, 2002; Wang & Tan, 2008; Ehrenstein & Gallaire, 2008). In figure 7, for the cases of 20, 40, 80, 120 and $200Hz$ a sequence of first two coupled modes and a third uncoupled mode is observed. For the cases 140, 160 and $180Hz$ and for the base non-actuated flow the uncoupled mode is instead the most energetic.

It can be seen that for all the actuated cases the first mode is less energetic than the non-actuated one. Thus, the

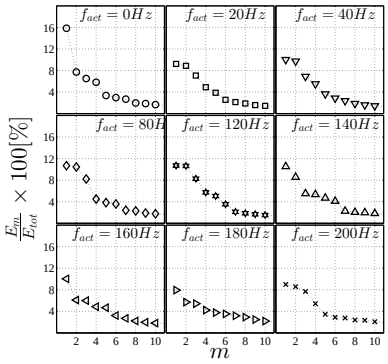

Figure 7. Normalised fluctuation energy of the first 10 modes. *m* indicates the mode number.

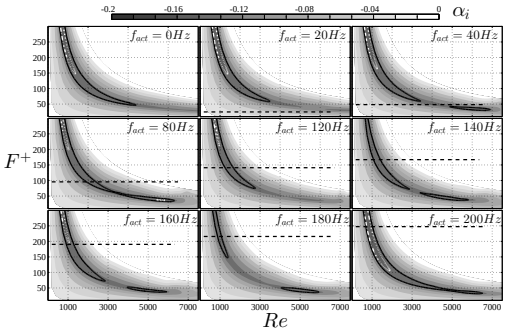

Figure 8. Stability diagrams for all investigated cases. Solid black line indicating the contour $\alpha_i = -0.12$. Dotted-dashed white line indicating the contour $\alpha_i = -0.135$. Dashed horizontal black lines indicates iso-frequency lines corresponding to the physical frequency of flow actuation. Stable region is left blank.

effect of periodically pulsed actuation is to redistribute the modal energy.

Linear Stability Theory Linear Stability Theory (LST) is employed in order to calculate the stability diagrams of the cases under investigation shown in figure 8. Non-dimensional frequency is given by equation 1

$$F^+ = \frac{2\pi f \nu}{\bar{U}^2} \times 10^5 \tag{1}$$

The stable and neutral part of the diagram is left blank. Arbitrary values of imaginary eigenvalue (α_i) were selected in order to facilitate the visualisation of the changes of the stability diagram among the different cases. Results indicate that the effect of the periodic pulsed disturbance introduced into the field of motion is able to change the stability of the flow itself verifying the previous experimental observations. It is evident that this kind of flow is already unstable for very low Reynolds number, as found in literature (Balsa, 1988; Lie & Riahi, 1988).

Given the shape of the stability diagram, higher actuation frequencies are able to stimulate more unstable frequencies at lower *Re* numbers, i.e. closer to the step. Therefore, higher frequencies are able to affect the flow more upstream. However, as the frequency of actuation is increased, values of negative imaginary part of the calculated eigenvalues decrease. According to the frequency of actuation, the perturbations generated by a pulsed input (Huerre & Monkewitz, 1985; Kaiktsis *et al.*, 1996) can drive an energy redistribution among the infinite modes (Ravindran, 2000; Couplet *et al.*, 2003) according to the new stability of the controlled flow. Therefore, a perturbed flow, reaching a new stability state, adapts itself to the periodic perturbation achieving a different mean flow with respect to the one of the non-actuated case.

CONCLUSIONS

A frequency analysis, POD and LST were carried out on time resolved PIV data. Results showed that the stability of actuated flows changed with respect to the base flow. Such behaviour indicated a Mean Flow Deformation (MFD) of the flow under control. The evolution of a periodically pulsed actuated flow is a strong function of the forcing frequency itself. The effect of the periodic pulsed perturbation which are convectively amplified downstream develop in large scale structures and promote transition from laminar to turbulent flow, in turn modifying the separated region. Due to the viscous-inviscid interaction (Smith, 1986; Sychev, 1998) the mean flow downstream of the transition location changes the overall pressure distribution across the field of motion affecting the flow also upstream. Therefore, a mean flow deformation is caused, which consequently changes the stability of the flow under control similar to the previous observations regarding laminar separation bubbles (Marxen & Rist, 2010).

The modified stability due to MFD (see figure 8) causes a redistribution of energy among the dominant modes, as POD analysis showed (see figure 7).

MFD is a consequence of the natural tendency of any physical perturbed system to a configuration of minimal energy. Therefore, a perturbed flow adapts itself to the periodic perturbation achieving a different mean flow with respect to the one of the non-actuated case, relaxing to new stability state.

Summarising, two main points are postulated: first, disturbances introduced by a pulsed periodical actuation drive the shear layer under control toward a modified stability behaviour. This is primarily an effect of MFD. Second, the most unstable frequency is a function of the local stream-wise location within the shear layer under control. This effectively means that the optimum actuation frequency for this type of convective flows is not the most amplified frequency at the location of the actuator but rather at the location of breakdown.

The implications of these two points need to be taken into account when reactive flow control strategies are designed towards controlling massively separated laminar shear layers. It becomes evident that the actuation frequency should be adjusted by means of a feedback loop in order to maximise the effectiveness of control based on the new stability state of the actuated flow. Additionally, the location of the actuator should be taken into account such that any forcing is tailored to arrive at the location of breakdown with the optimum spectral content.

REFERENCES

Armaly, B.F., Durst, F., Pereira, J.C.F. & Schoenung, B. 1983 Experimental and theoretical investigation of backward-facing step flow. *Journal of Fluid Mechanics* **127**, 473–496.

Balsa, Thomas F. 1988 On the receptivity of free shear layers to two-dimensional external excitation. *Journal of Fluid Mechanics* **187**, 155–177.

Bechert, D. W. & Stahl, B. 1988 Excitation of instability waves in free shear layers part 2. experiments. *Journal of Fluid Mechanics* **186**, 63–84.

Bhattacharjee, S., Scheelke, B. & Troutt, T.R. 1986 Modification of vortex interactions in a reattaching separated flow. *AIAA journal* **24** (4), 623–629.

Blackburn, H.M., Barkley, D. & Sherwin, S.J. 2008 Convective instability and transient growth in flow over a backward-facing step. *Journal of Fluid Mechanics* **603**, 271–304.

Bradshaw, P. & Wong, F. Y. F. 1972 The reattachment and relaxation of a turbulent shear layer. *Journal of Fluid Mechanics* **52**, 113–135.

Chun, K.B. & Sung, H.J. 1996 Control of turbulent separated flow over a backward-facing step by local forcing. *Experiments in Fluids* **21** (6), 417–426.

Correale, G., Michelis, T., Ragni, D., Kotsonis, M. & Scarano, F. 2014 Nanosecond-pulsed plasma actuation in quiescent air and laminar boundary layer. *Journal of Physics D: Applied Physics* **47** (10), XX.

Couplet, M., SAGAUT, P. & BASDEVANT, C. 2003 Intermodal energy transfers in a proper orthogonal decomposition galerkin representation of a turbulent separated flow. *Journal of Fluid Mechanics* **491**, 275–284.

Deane, A.E., Kevrekidis, I.G., Karniadakis, G.E. & Orszag, S.A. 1991 Low-dimensional models for complex geometry flows: Application to grooved channels and circular cylinders. *Physics of Fluids A* **3** (10), 2337–2354.

Eaton, John K. & Johnston, James P. 1981 Review of research on subsonic turbulent flow reattachment. **19** (9), 1093–1100.

Ehrenstein, U. & Gallaire, F. 2008 Two-dimensional global low-frequency oscillations in a separating boundary-layer flow **614**, 315–327.

Farrell, Brian F. 1988 Optimal excitation of perturbations in viscous shear flow. *Physics of Fluids (1958-1988)* **31** (8), 2093–2102.

Gudmundsson, K. & Colonius, T. 2011 Instability wave models for the near-field fluctuations of turbulent jets **689**, 97–128.

Hasan, M.A.Z. 1992 The flow over a backward-facing step under controlled perturbation: laminar separation. *Journal of Fluid Mechanics* **238**, 73–96.

Huerre, P. & Monkewitz, P.A. 1985 Absolute and convective instabilities in free shear layers. *Journal of Fluid Mechanics* **159**, 151–168.

Kaiktsis, L., Karniadakis, G.E.M. & Orszag, S.A. 1996 Unsteadiness and convective instabilities in two-dimensional flow over a backward-facing step. *Journal of Fluid Mechanics* **321**, 157–187.

Kaiktsis, Lambros, Karniadakis, George E.M. & Orszag, Steven A. 1991 Onset of three-dimensionality, equilibria, and early transition in flow over a backward-facing step. *Journal of Fluid Mechanics* **231**, 501–528.

Kim, J., Kline, S.J. & Johnston, J.P. 1980 Investigation of a reattaching turbulent shear layer: flow over a backward-facing step. *Journal of Fluids Engineering, Transactions of the ASME* **102** (3), 302–308.

Lie, K.H. & Riahi, D.N. 1988 Numerical solution of the orr-sommerfeld equation for mixing layers. *International Journal of Engineering Science* **26** (2), 163–174.

Lin, N, Reed, HL & Saric, WS 1992 Effect of leading-edge geometry on boundary-layer receptivity to freestream sound. In *Instability, Transition, and Turbulence* (ed. M.Y. Hussaini, A. Kumar & C.L. Streett), pp. 421–440. Springer New York.

Marxen, Olaf 2005 *Numerical studies of physical effects related to the controlled transition process in laminar separation bubbles*. na.

Marxen, O. & Rist, U. 2010 Mean flow deformation in a laminar separation bubble: Separation and stability characteristics **660**, 37–54.

Michalke, A 1965 On spatially growing disturbances in an inviscid shear layer. *Journal of Fluid Mechanics* **23** (3), 521–544.

Monkewitz, P.A. & Huerre, P. 1982 Influence of the velocity ratio on the spatial instability of mixing layers. *Physics of Fluids* **25** (7), 1137–1143.

Orszag, Steven A. 1971 Accurate solution of the orr-sommerfeld stability equation. *Journal of Fluid Mechanics* **50**, 689–703.

Price, S.J., Sumner, D., Smith, J.G., Leong, K. & Padoussis, M.P. 2002 Flow visualization around a circular cylinder near to a plane wall **16** (2), 175–191.

Ravindran, S.S. 2000 A reduced-order approach for optimal control of fluids using proper orthogonal decomposition **34** (5), 425–448.

Rist, Ulrich, Maucher, Ulrich & Wagner, Siegfried 1996 Direct numerical simulation of some fundamental problems related to transition in laminar separation bubbles. *Computational Methods in Applied Sciences* **96**, 319–325.

Roos, Frederick, Kegelman, W. & T., Jerome 1986 Control of coherent structures in reattaching laminar and turbulent shear layers. *AIAA journal* **24** (12), 1956–1963.

Sirovich, L. 1987*a* Turbulence and the dynamics of coherent structures. I - Coherent structures. *Quarterly of Applied Mathematics* **45**, 561–571.

Sirovich, L. 1987*b* Turbulence and the dynamics of coherent structures. II - Symmetries and transformations. . *Quarterly of Applied Mathematics* **45**, 561–571.

Sirovich, L. 1987*c* Turbulence and the dynamics of coherent structures. III - Dynamics and scaling. *Quarterly of Applied Mathematics* **45**, 561–571.

Smith, FT 1986 Steady and unsteady boundary-layer separation. *Annual review of fluid mechanics* **18** (1), 197–220.

Sychev, Vladimir V 1998 *Asymptotic theory of separated flows*. Cambridge University Press.

Van Ingen, J. & Kotsonis, M. 2011 A two-parameter method for en transition prediction.

Van Oudheusden, B.W., Scarano, F., Van Hinsberg, N.P. & Watt, D.W. 2005 Phase-resolved characterization of vortex shedding in the near wake of a square-section cylinder at incidence. *Experiments in Fluids* **39** (1), 86–98.

Wang, X.K. & Tan, S.K. 2008 Near-wake flow characteristics of a circular cylinder close to a wall **24** (5), 605–627.

Wengle, Hans, Huppertz, Andr, Brwolff, Gnter & Janke, Gerd 2001 The manipulated transitional backward-facing step flow: an experimental and direct numerical simulation investigation. *European Journal of Mechanics - B/Fluids* **20** (1), 25 – 46.